

## TRANSFUSION MEDICINE

# Osteopontin mediates murine transfusion-related acute lung injury via stimulation of pulmonary neutrophil accumulation

Rick Kapur,<sup>1</sup> Gopinath Kasetty,<sup>2</sup> Johan Rebetz,<sup>1</sup> Arne Egesten,<sup>2,3</sup> and John W. Semple<sup>1,3,4</sup>

<sup>1</sup>Division of Hematology and Transfusion Medicine, Department of Laboratory Medicine and <sup>2</sup>Respiratory Medicine and Allergology, Lund University, Lund, Sweden; <sup>3</sup>Skåne University Hospital, Lund, Sweden; and <sup>4</sup>Department of Pharmacology, University of Toronto, Toronto, ON, Canada

## KEY POINTS

- OPN localizes to the lung and is critically required for induction of murine TRALI via stimulation of pulmonary PMN accumulation.
- The OPN-mediated murine TRALI response is dependent on macrophages and OPN polymerization and is independent from CD44, MIP-2, and IL-6.

**Transfusion-related acute lung injury (TRALI) is one of the leading causes of transfusion-related fatalities and is characterized by the onset of acute respiratory distress within 6 hours upon blood transfusion. Specific therapies are unavailable. Preexisting inflammation is a risk factor for TRALI and neutrophils (polymorphonuclear neutrophils [PMNs]) are considered to be the major pathogenic cells. Osteopontin (OPN) is a multifunctional protein expressed at sites of inflammation and, for example, is involved in pulmonary disorders, can regulate cellular migration, and can function as a PMN chemoattractant. We investigated whether OPN is involved in TRALI induction by promoting PMN recruitment to the lungs. Using a previously established murine TRALI model, we found that in contrast to wild-type (WT) mice, OPN knockout (KO) mice were resistant to antibody-mediated PMN-dependent TRALI induction. Administration of purified OPN to the OPN KO mice, however, restored the TRALI response and pulmonary PMN accumulation. Alternatively, blockade of OPN in WT mice using an anti-OPN antibody prevented the onset of TRALI induction. Using pulmonary immunohistochemistry, OPN could be specifically detected in the lungs of mice that suffered from TRALI. The OPN-mediated**

**TRALI response seemed dependent on macrophages, likely the cellular source of OPN and OPN polymerization, and independent from the OPN receptor CD44, interleukin 6 (IL-6), and other PMN chemoattractants including macrophage inflammatory protein-2 (MIP-2). These data indicate that OPN is critically required for induction of antibody-mediated murine TRALI through localization to the lungs and stimulation of pulmonary PMN recruitment. This suggests that anti-OPN antibody therapy may be a potential therapeutic strategy to explore in TRALI patients. (*Blood*. 2019;134(1):74-84)**

## Introduction

Transfusion-related acute lung injury (TRALI) is a life-threatening syndrome that occurs within 6 hours of a blood transfusion and is characterized by the onset of acute respiratory distress and the development of noncardiogenic pulmonary edema.<sup>1</sup> TRALI is one of the leading causes of transfusion-related fatalities and specific therapies are not available.<sup>1,2</sup> The pathophysiology of TRALI is complex and a better understanding is highly warranted.<sup>1</sup> Polymorphonuclear neutrophils [PMNs] have been recognized as the major pathogenic cells in the pathophysiology of TRALI<sup>1-3</sup> whereas CD4<sup>+</sup>CD25<sup>+</sup>FoxP3<sup>+</sup> T-regulatory cells and dendritic cells are major protective cells against TRALI induction.<sup>1,4</sup> TRALI pathology can be viewed as a 2-hit model,<sup>1,5,6</sup> where the first hit represents the underlying clinical condition of the patient (eg, inflammation) and the second hit is conveyed by the transfusion product containing pathogenic antileukocyte antibodies<sup>1,7</sup> and/or biological response modifiers (eg, lipids).<sup>1,8</sup> The nature of the inflammation in TRALI patients is evident from increased

levels of the proinflammatory cytokines interleukin-6 (IL-6) and IL-8<sup>9,10</sup> as well as the acute-phase protein C-reactive protein,<sup>11</sup> which is a diagnostic marker for acute infections and inflammation.<sup>12</sup> C-reactive protein was also shown to functionally enable antibody-mediated murine TRALI via synergistically enhancing pulmonary PMN recruitment together with the TRALI-inducing antibodies.<sup>13</sup>

Osteopontin (OPN) is a matricellular protein with multiple biological functions.<sup>14</sup> These functions include both normal physiological processes (eg, regulating bone tissue biomineralization and restricting the growth of calcium crystals in epithelial tissues)<sup>15</sup> as well as pathological processes in various disease states such as cancer, atherosclerosis, glomerulonephritis, and several chronic inflammatory diseases.<sup>16</sup> OPN can function as an important proinflammatory cytokine and is able to regulate cellular adhesion and migration of various immune cells including PMNs.<sup>16</sup> Interestingly, OPN has also been shown to be abundantly expressed

in multiple lung diseases, regulating aspects of pulmonary granuloma formation, lung fibrosis, and lung carcinoma.<sup>17</sup> Additionally, OPN is upregulated at sites of inflammation and tissue remodeling.<sup>18,19</sup>

As the pathophysiology of TRALI involves inflammation and pulmonary PMN migration, we hypothesized that OPN may play a role in the onset of TRALI as a pulmonary PMN chemoattractant. We therefore investigated the involvement of OPN in TRALI by using our previously established murine TRALI model, which is based on low-dose lipopolysaccharide (LPS) priming (when mice are housed in a specific pathogen-free [SPF] setting) and CD4<sup>+</sup> T-cell depletion, followed by injection of anti-major histocompatibility complex (MHC) class I antibodies.<sup>4,20</sup> The results suggest that OPN is critically involved in the development of antibody-mediated TRALI by attracting PMNs toward the lungs and that blocking OPN using anti-OPN antibodies may be a promising potential therapeutic intervention for TRALI.

## Methods

### Mice

C57BL/6 (H-2b, C57BL/6NCr) wild-type (WT) mice were obtained from Charles River Laboratories (Sulzfeld, Germany) and C57BL/6 OPN knockout (KO) mice were bred and genotyped at Lund University (Lund, Sweden). All mice were males, 8 to 10 weeks of age, and were housed under SPF conditions for at least 1 week in the animal facility at the Biomedical Service Division at Lund University before initiating experiments. Both WT and KO mice demonstrated similar levels of PMNs in bone marrow and whole blood (supplemental Figure 1, available on the *Blood* Web site), as measured on the Sysmex XN-350 (Kungsbacka, Sweden). All animal studies were approved by the animal ethics committee of Lund University in accordance with the guidelines of the Swedish National Board of Agriculture and the European Union directive for the protection of animals used in science.

### Antibodies and reagents

Antibodies for induction of TRALI in mice were 3A-1-2s (monoclonal mouse immunoglobulin G2a [IgG2a], which reacts with murine H-2Kd and H-2Dd MHC class I molecules) and AF6-88.5.5.3 (monoclonal mouse IgG2a, which reacts to murine MHC class I H-2Kb), as well as the *in vivo* CD4<sup>+</sup> T-cell-depleting antibody GK1.5 (anti-CD4, rat IgG2b) and the anti-mouse/human CD44 antibody IM7 and its isotype control rat IgG2b LTF-2, all purchased from Bio X Cell (West Lebanon, NH). BM-8 (anti-mouse F4/80-fluorescein isothiocyanate) was purchased from BioLegend (San Diego, CA). RM4-5 (anti-mouse CD4-phycoerythrin) was purchased from BD Pharmingen (San Diego, CA). For OPN-immunohistochemistry staining, rabbit anti-mouse OPN (clone O-17) was purchased from IBL International (Gunma, Japan) and F(ab')<sub>2</sub> donkey anti-rabbit IgG (H+L)-horseradish peroxidase (HRP)-conjugated was purchased from Jackson ImmunoResearch (West Grove, PA). Anti-OPN antibody, normal goat IgG isotype control antibody, and recombinant mouse OPN were purchased from R&D Systems (Minneapolis, MN). LPS (*Escherichia coli* O55:B5) and cystamine dihydrochloride were obtained from Sigma-Aldrich Sweden AB (Stockholm, Sweden). Clodronate liposomes were purchased from Liposoma (Amsterdam, The Netherlands).

### Antibody-mediated murine TRALI model

TRALI was induced as previously described.<sup>4,20</sup> Briefly, 18 hours before TRALI induction, mice were primed with 0.1 mg/kg LPS intraperitoneally and injected intraperitoneally with the monoclonal antibody GK1.5 (4.5 mg/kg) to deplete CD4<sup>+</sup> T cells. In indicated experiments, mice were additionally treated with 200  $\mu$ L of clodronate liposomes intraperitoneally 4 days and 18 hours before TRALI induction. On the day of the experiment, LPS-primed and CD4-depleted (and in indicated experiments also macrophage-depleted) mice were injected IV with 600  $\mu$ L of a mixture of the TRALI-inducing antibodies 3A-1-2s (45 mg/kg) and AF6-88.5.5.3 (4.5 mg/kg) with or without addition of the indicated treatments including recombinant OPN (0.9 mg/kg), isotype antibody (normal goat IgG), anti-OPN antibody (2.25 mg/kg), anti-CD44 antibody IM7 (9 mg/kg), rat IgG2b isotype control LTF-2, and cystamine (50 mg/kg). Subsequently, rectal temperatures were taken every 30 minutes (up to 90 minutes) using a RET-3 rectal probe for mice (VWR International, Mississauga, ON, Canada) connected to a traceable digital thermometer (Physitemp Instruments, Inc, Clifton, NJ). Ninety minutes after TRALI initiation, mice were anesthetized with a mixture of ketamine and rompun and exsanguinated by cardiac puncture with blood drawn into 100  $\mu$ L of phosphate-buffered saline (PBS)/citrate phosphate dextrose adenine.

### Tissue processing

After the mice were euthanized, the left lung and spleen were harvested and single-cell suspensions were made by manual homogenization of the tissues in PBS/citrate phosphate dextrose adenine followed by transfer of the cells through a 40- $\mu$ M cell strainer (BD Biosciences, Bedford, MA). Red blood cells in the filtered solution were lysed by addition of 14 mL of an ammonium chloride/potassium bicarbonate lysis solution (0.15 M NH<sub>4</sub>Cl, 10 mM KHCO<sub>3</sub>, Na<sub>2</sub>EDTA; pH 7.2-7.4) for 7 minutes on ice and washed with PBS. The spleen cells were used to verify CD4<sup>+</sup> T-cell depletion by flow cytometry.

### Lung W/D weight ratios

Lung wet/dry (W/D) weight ratios, a direct measure of pulmonary edema, were determined as previously described.<sup>4,13,20</sup> Briefly, the right lung of each mouse was removed and weighed to determine the wet weight and then dried in an oven for 48 hours at 60°C. The dried lung tissues were reweighed to obtain the dry weight. The lung W/D weight ratio was calculated by the formula: net wet weight/net dry weight.

### Pulmonary PMN enumeration

The red blood cell-lysed lung cell suspensions were centrifuged onto microscope slides (Superfrost Plus; Fisher Scientific, Pittsburgh, PA) using a Centurion Scientific PrO-Cyt LCD centrifuge (Chichester, United Kingdom) followed by staining with Hemacolor rapid staining of the blood smear staining kit for microscopy (Merck KGaA, Darmstadt, Germany). The slides were mounted with Neo-Mount (Merck KGaA) and imaged using an Olympus BX60F microscope with an SC50 camera in a blinded manner. All nucleated cells were scored in 4 randomly selected and nonoverlapping fields using ImageJ software, and the pulmonary PMN percentage was obtained by the formula: average number of observed PMN (in 4 fields)/average number of nucleated cells (in 4 fields)  $\times$  100.

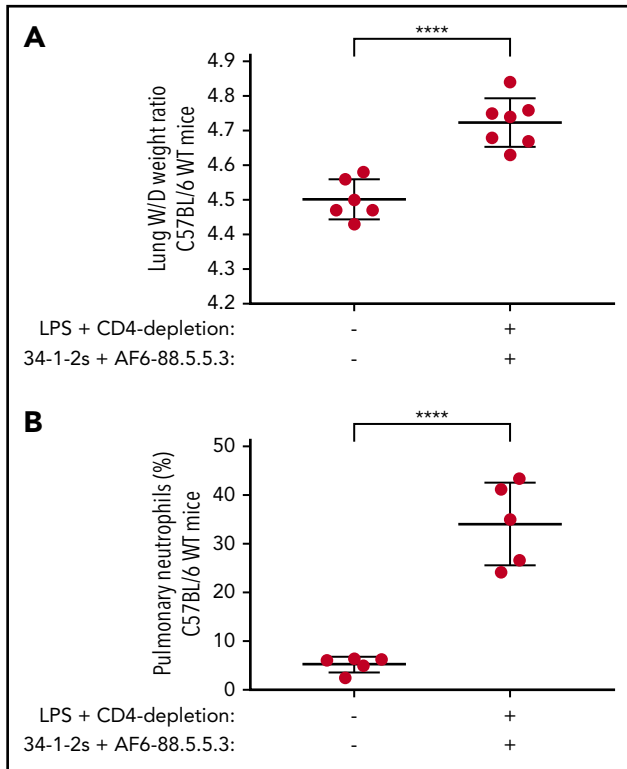


**Figure 1. Antibody-mediated TRALI is associated with increased pulmonary PMN accumulation in WT mice.** Lung W/D weight ratios (A) and percentage of pulmonary PMNs (B) in C57BL/6 WT mice primed with LPS, depleted of CD4<sup>+</sup> T cells, and injected (or not) with anti-MHC class I antibodies (clones 34-1-2s and AF6-88.5.5.3). Statistical analysis was performed with a 1-tailed unpaired Student t test. Each dot represents 1 mouse and error bars represent SD. \*\*\*\**P* < .0001.

### Lung tissue histology and immunohistochemistry

A segment of the left lung was fixed in Histofix (Histolab Products AB, Askim, Sweden) and embedded into paraffin and sectioned (3  $\mu$ m) with a microtome. The tissue sections were placed on slides (Superfrost Plus; Fisher Scientific) and deparaffinized in serial baths of xylene and ethanol followed by staining using Mayer hematoxylin and 0.2% eosin (Histolab Products AB, Askim, Sweden) or immunohistochemistry staining. Lung histology was quantitatively scored for lung injury as previously described.<sup>21</sup> For the immunohistochemistry staining of OPN, endogenous peroxidase was blocked with 3% H<sub>2</sub>O<sub>2</sub> (Boster Biological technology, Pleasanton, CA) followed by heat-induced epitope retrieval in citrate buffer pH6 (Boster Biological Technology, Pleasanton, CA). Subsequently, blocking was performed using 5% bovine serum albumin and 0.05% Triton-X 100 (Sigma-Aldrich Chemie GmbH, Steinheim, Germany) in PBS (Medicago AB, Uppsala, Sweden) and the primary antibody rabbit anti-mouse OPN (clone: 0-17; IBL International) was incubated at 10  $\mu$ g/mL overnight at 4°C. The slides were washed in PBS and incubated with the secondary antibody F(ab')<sub>2</sub> donkey anti-rabbit IgG (H+L)-HRP-conjugated (Jackson ImmunoResearch) at a 1/2000 dilution for 45 minutes at room temperature. Tissue sections were stained with a DAB Chromogenic Substrate kit (Boster Biological Technology) according to the manufacturer's instructions. The slides were counterstained with Mayer hematoxylin (Histolab Products AB) and mounted with Neo-Mount (Merck KGaA). The stained

slides were imaged using an Olympus BX60F microscope with an SC50 camera.

### Cytokine measurements

Blood obtained via cardiac puncture was centrifuged at 2500g for 15 minutes (without brake) and plasma was collected, aliquoted, and stored at -80°C for subsequent batch analysis. The thawed plasma was analyzed for murine macrophage inflammatory protein-2 (MIP-2) or OPN levels using solid-phase sandwich enzyme-linked immunosorbent assay (ELISA) kits: the mouse CXCL2/MIP-2 Quantikine ELISA kit or mouse OPN ELISA DuoSet, respectively (R&D Systems). Additionally, other mentioned cytokines, including IL-6, were evaluated using the Bio-Plex Pro Mouse Cytokine 23-plex assay (Bio-Rad, Hercules, CA). All ELISAs were performed according to the manufacturer's protocol.

### Statistical analysis

All hypotheses were made before initiation of an experiment and it was predecided whether 1-tailed or 2-tailed statistical testing

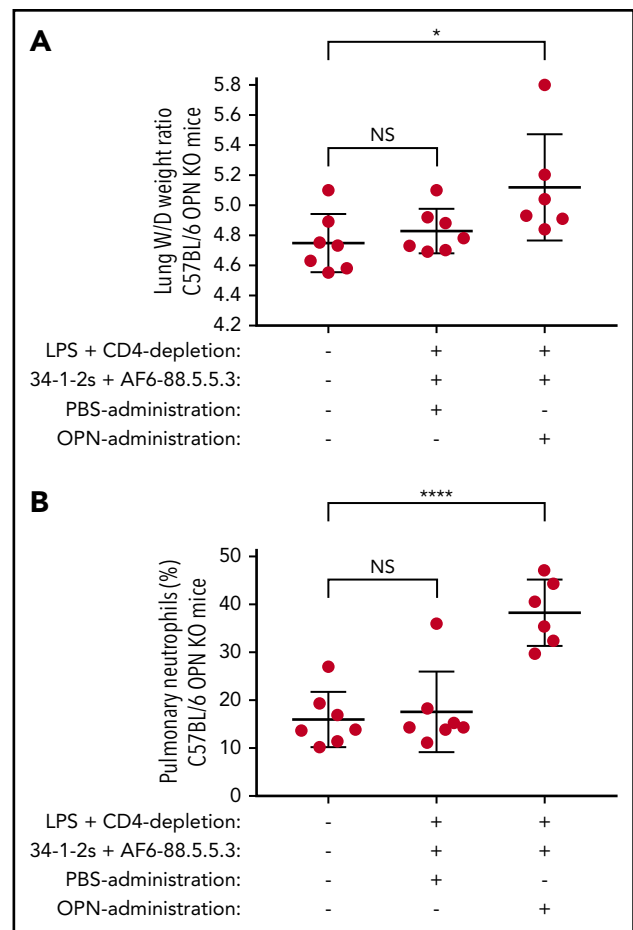


**Figure 2. OPN KO mice are resistant to antibody-mediated TRALI, however, OPN administration restores PMN-dependent antibody-mediated TRALI.** Lung W/D weight ratios (A) and percentage of pulmonary PMNs (B) in C57BL/6 OPN KO mice primed with LPS, depleted of CD4<sup>+</sup> T cells, and injected with anti-MHC class I antibodies (clones 34-1-2s and AF6-88.5.5.3) and either PBS or OPN. For statistical analyses, only significant comparisons of interest are shown. Statistical analysis was performed with a 1-way analysis of variance (ANOVA) with a Tukey post hoc test. Each dot represents 1 mouse and error bars represent SD. \**P* < .05, \*\*\*\**P* < .0001. NS, nonsignificant.

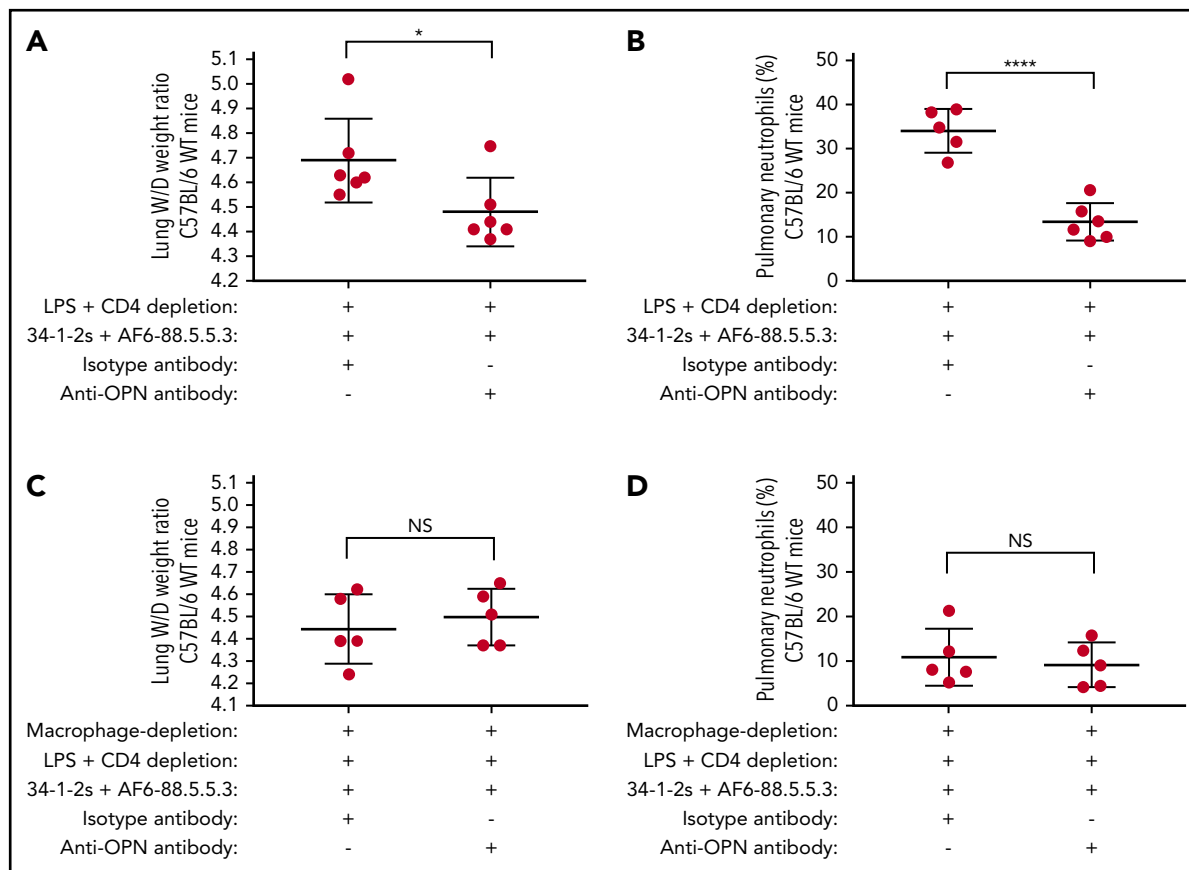


**Figure 3. Blockade of OPN in WT mice or macrophage depletion prevents the occurrence of PMN-dependent antibody-mediated TRALI in C57BL/6 WT mice.** Lung W/D weight ratios (A,C) and percentage of pulmonary PMNs (B,D) in C57BL/6 WT mice primed with LPS, depleted of CD4<sup>+</sup> T cells, injected with anti-MHC class I antibodies (clones 34-1-2s and AF6-88.5.5.3), either isotype-control antibody or anti-OPN antibody, and depleted of macrophages (C-D) or not (A-B). Statistical analysis was performed with a 1-tailed unpaired Student t test. Each dot represents 1 mouse, and error bars represent SD. \* $P < .05$ , \*\*\*\* $P < .0001$ .

would be applied. Normal distribution was evaluated and consequently the appropriate (non)parametric statistical tests were selected. Statistical analysis was carried out using GraphPad Prism 7.04 software for Windows (GraphPad Software, San Diego, CA) with statistical significance set at  $P < .05$ . The specific statistical tests used are mentioned in the figure legends. All error bars in the manuscript represent standard deviation (SD).

## Results

### OPN KO mice are resistant to antibody-mediated PMN-dependent TRALI

We first validated our previously established murine C57BL/6 TRALI model,<sup>4,20</sup> by priming the SPF-housed mice with low-dose LPS and depleting their CD4<sup>+</sup> T cells, prior to initiating TRALI with infusion of anti-MHC class I antibodies (34-1-2s and AF6-88.5.5.3). Compared with untreated mice, C57BL/6 WT mice suffered from antibody-mediated TRALI as shown by their significantly increased lung W/D weight ratio (4.72 vs 4.50, respectively;  $P < .0001$ ; Figure 1A). This also corresponded to significantly increased levels of pulmonary PMNs compared with untreated naive mice (34% vs 5%;  $P < .0001$ ; Figure 1B). In contrast to the WT mice, however, C57BL/6 OPN (KO) mice were resistant to antibody-mediated TRALI induction as they did not

display any significant increase in lung W/D levels or pulmonary PMN accumulation compared with naive OPN KO mice (lung W/Ds, 4.83 vs 4.75, and pulmonary PMNs, 18% vs 16%, respectively; Figure 2).

### OPN administration restores TRALI responses in OPN KO mice

Administration of recombinant OPN to OPN KO mice significantly induced TRALI reactions compared with untreated naive OPN KO mice (lung W/Ds, 5.12 vs 4.75;  $P < .05$ ; Figure 2A). The TRALI-inducing effect of OPN administration to OPN KO mice was associated with increased levels of pulmonary PMNs (38% vs 16% compared with untreated naive OPN KO;  $P < .0001$ ; Figure 2B).

### OPN blockade with an anti-OPN antibody prevents TRALI in WT mice

Alternatively, in vivo blocking of OPN in WT mice by administration of an anti-OPN antibody demonstrated decreased lung W/Ds as compared with treatment with an isotype antibody (4.48 vs 4.69, respectively;  $P < .05$ ; Figure 3A). The OPN-blocking response during TRALI was associated with a decreased level of pulmonary PMN accumulation as compared with treatment with an isotype antibody (14% vs 34%, respectively;  $P < .0001$ ; Figure 3B).

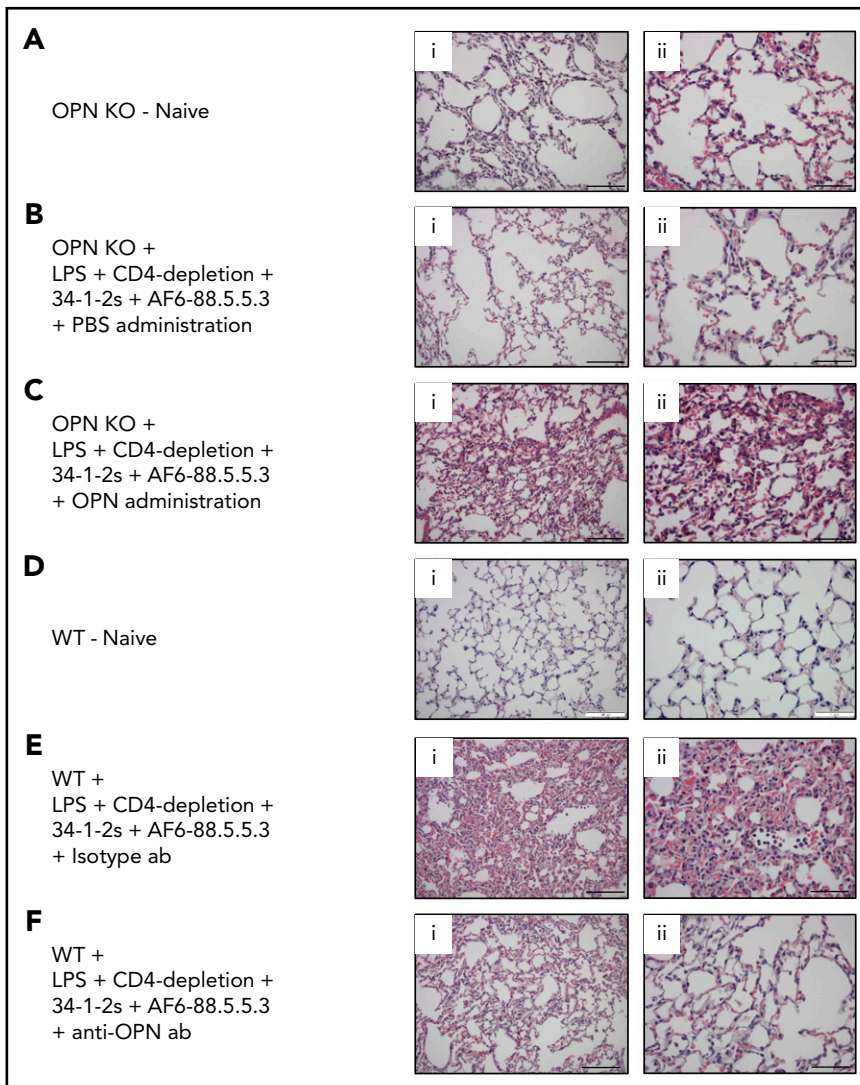


**Figure 4. Lung tissue histology of OPN-related TRALI responses.** (A-F) Histology performed on lung tissue from the indicated mouse groups. (i-ii) H&E-stained lung tissue images taken at original magnification (i)  $\times 20$  and (ii)  $\times 40$ . Representative images of each indicated group are shown. Scale bars, (i) 100  $\mu\text{m}$  and (ii) 50  $\mu\text{m}$ . ab, antibody.

### Macrophage depletion prevents PMN-dependent TRALI in WT mice

To assess the role of macrophages in TRALI, we depleted macrophages in WT mice using clodronate liposomes (supplemental Figure 2). Subsequently, we induced TRALI by LPS priming and CD4<sup>+</sup> T-cell depletion followed by infusion of TRALI antibodies, with co-infusion of either isotype antibody or anti-OPN antibody. When macrophages were depleted, no TRALI occurred as there was no significant difference in lung W/Ds with the co-infusion of isotype antibody vs anti-OPN antibody (Figure 3C). Accordingly, when macrophages were depleted and TRALI was induced, there was also no significant difference in pulmonary PMN numbers upon co-infusion of isotype antibody vs anti-OPN antibody (Figure 3D). This supports a pathogenic role for macrophages in PMN-dependent antibody-mediated TRALI.

### OPN induces lung tissue damage in antibody-mediated PMN-dependent TRALI

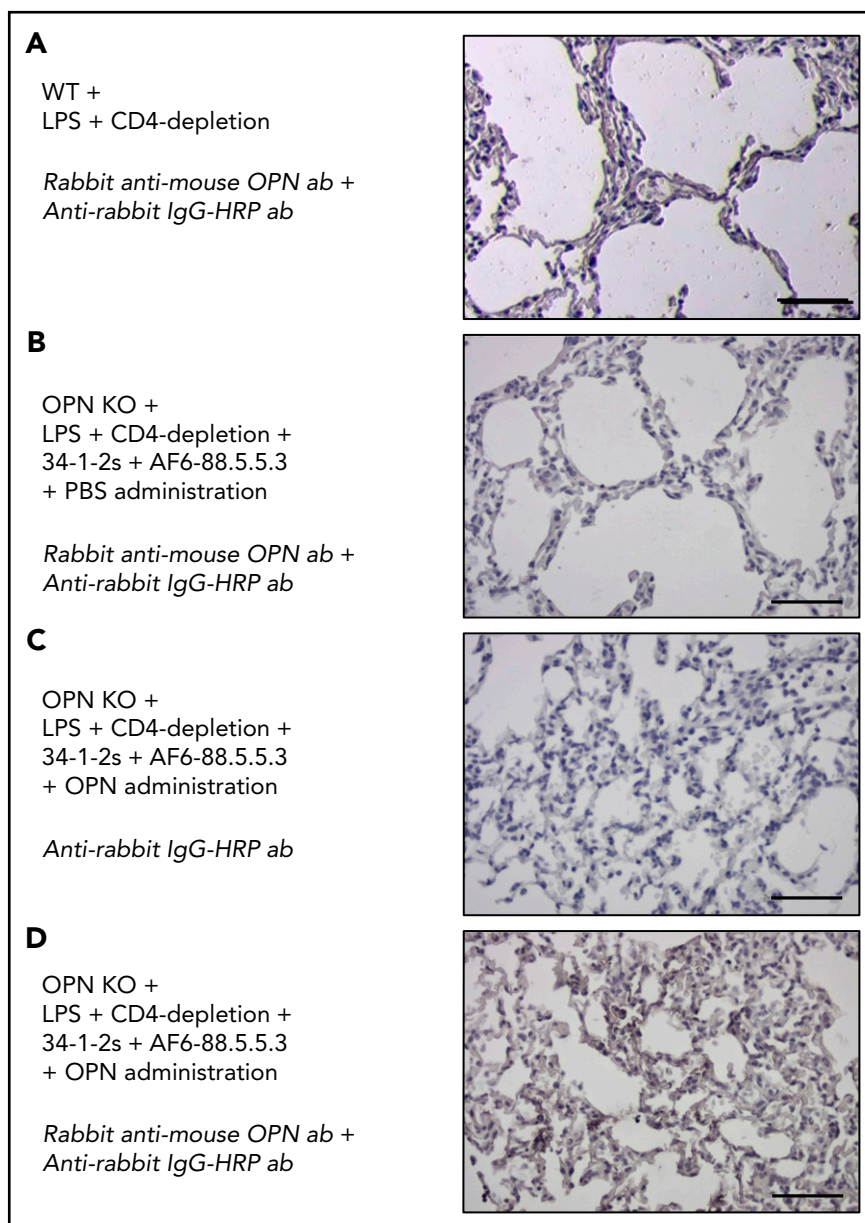
We next verified the acute lung injury in the various treatment groups by performing lung tissue histology analyses. Compared with naive or PBS-injected control mice (Figure 4A-B,

respectively), we observed signs of severe antibody-mediated acute lung injury (increased alveolar septal thickening, exudates indicating edema and intra-alveolar PMN infiltration) in the OPN KO mice injected with recombinant OPN (Figure 4C). On the other hand, no signs of antibody-mediated acute lung injury were observed in WT mice injected with anti-OPN antibody (Figure 4F) or in naive control mice (Figure 4D) in contrast to isotype antibody-injected WT mice, which demonstrated severe acute lung injury (Figure 4E). These data were in full agreement with a quantitative assessment according to the recommended published guidelines for experimental acute lung injury in animals.<sup>21</sup> (supplemental Figure 3).

### Increased pulmonary OPN levels are present in mice suffering from TRALI

As the TRALI-inducing effect of OPN administration corresponded to increased numbers of pulmonary PMNs and OPN is known to regulate recruitment and migration of PMNs,<sup>22</sup> we performed lung immunohistochemistry to investigate lung OPN levels during TRALI. In OPN KO mice, which suffered from TRALI due to administration of OPN, we could specifically detect the presence of OPN in the lungs (Figure 5D). This pulmonary

**Figure 5. OPN is present in murine TRALI lungs.** (A-D) Detection of OPN in the lungs using immunohistochemistry in the indicated mouse groups. Panels on the right represent lung tissue images taken at original magnification  $\times 40$  with specific antibody stain after the indicated immunohistochemistry treatments. Scale bars, 50  $\mu\text{m}$ .



staining of OPN did not occur upon LPS priming and CD4<sup>+</sup> T-cell depletion (Figure 5A) and was specific to TRALI lungs as also no OPN was detected in the lungs of TRALI-resistant OPN KO mice (Figure 5B) or in lungs using the secondary antibody alone for staining (Figure 5C).

### Plasma OPN levels are low during TRALI but increase upon TRALI prevention with anti-OPN antibody treatment

As we could specifically detect OPN in TRALI lungs, we investigated whether the OPN levels in the plasma would be low during TRALI. We observed that upon TRALI induction, plasma OPN levels were low, however, when TRALI was prevented by anti-OPN antibody treatment, the levels of OPN in the plasma significantly increased as compared with isotype antibody treatment (62 vs 34 ng/mL;  $P < .0001$ ; Figure 6A). Notably, there was no significant difference in plasma OPN levels of naive mice

compared with mice depleted of CD4<sup>+</sup> T cells and/or primed with low-dose LPS (Figure 6A).

### Macrophages are the likely source of OPN during TRALI

When macrophages were depleted in vivo and TRALI was prevented by anti-OPN antibody treatment, the levels of plasma OPN were significantly lower as compared with when macrophages were undepleted (37 vs 62 ng/mL;  $P < .0001$ ; Figure 6A), suggesting that macrophages may be the source of OPN during TRALI.

### OPN polymerization appears to be required for PMN-dependent antibody-mediated TRALI, unlike CD44

To investigate the contribution of OPN polymerization in the induction of TRALI, we inhibited the polymerization in vivo using

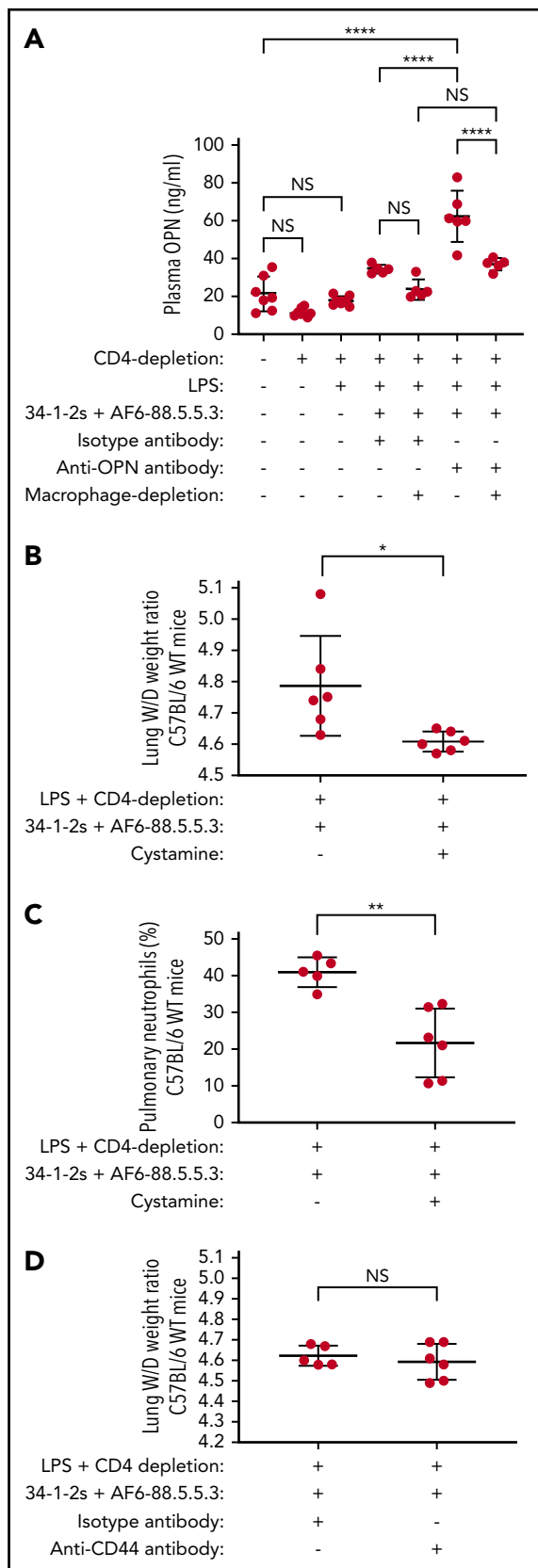


**Figure 6. Plasma OPN levels are low during TRALI, increase upon TRALI prevention by OPN blockade with levels remaining low when macrophages are depleted, and treatment with cystamine but not with anti-CD44 antibody prevents antibody-mediated PMN-dependent TRALI.** Plasma OPN levels in

cystamine. Administration of cystamine prevented the onset of TRALI compared with untreated TRALI mice (lung W/Ds, 4.60 vs 4.79;  $P < .05$ ; Figure 6B). This effect of cystamine treatment was also associated with decreased levels of pulmonary PMNs as compared with untreated TRALI mice (22% vs 41%;  $P < .01$ , Figure 6C). Next, we examined whether the leukocyte OPN receptor CD44 was involved in the TRALI response. For that purpose, we blocked CD44 in the murine TRALI model using an anti-CD44 antibody. Blocking CD44, however, did not affect the TRALI response as compared with an isotype antibody (Figure 6D), suggesting that OPN does not engage CD44 in the mediation of antibody-mediated PMN-dependent TRALI.

### OPN-induced PMN-dependent antibody-mediated TRALI responses are independent of both MIP-2 and IL-6

As the PMN chemoattractant MIP-2 has previously been described to be upregulated in murine antibody-mediated TRALI,<sup>4,13,20,23,24</sup> we determined whether the ability of OPN to induce antibody-mediated PMN-dependent TRALI was related to the levels of MIP-2. We found that compared with naive controls, plasma MIP-2 levels were significantly increased in mice that were infused with the TRALI-inducing antibodies (Figure 7A-B), however, injection or blocking of OPN did not affect the high MIP-2 levels (Figure 7A-B). This indicates that the OPN-related PMN response in TRALI is a distinct mechanism that is independent of plasma MIP-2 levels.

Similarly, we investigated whether the ability of OPN to induce antibody-mediated PMN-dependent TRALI was related to the levels of IL-6, also known to be increased in TRALI patients.<sup>9,10</sup> Compared with naive controls, plasma IL-6 levels were significantly increased in mice that were infused with the TRALI-inducing antibodies (Figure 7C-D), however, injection or blocking of OPN did not affect the high IL-6 levels (Figure 7C-D). This also indicates that the OPN-related PMN response in TRALI is a distinct mechanism unrelated to plasma IL-6 levels.

We also assessed whether other PMN chemoattractant cytokines could be involved in antibody-mediated TRALI induction by OPN. We measured plasma levels of granulocyte-macrophage colony-stimulating factor (GM-CSF), granulocyte colony-stimulating factor (G-CSF), interferon- $\gamma$ , keratinocyte chemoattractant (KC), monocyte chemoattractant protein-1 (MCP-1), MIP-1 $\alpha$ , MIP-1 $\beta$ , regulated upon activation normal T-cell expressed and secreted (RANTES), and tumor necrosis factor- $\alpha$  (TNF)- $\alpha$  in OPN KO mice administered OPN (supplemental Figure 4) and in WT mice treated with anti-OPN antibody (supplemental Figure 5). Compared with naive controls, infusion of TRALI antibodies into OPN KO mice significantly increased the plasma levels of GM-CSF,

**Figure 6 (continued)** C57BL/6 WT mice primed with LPS and/or depleted of CD4<sup>+</sup> T cells, injected with anti-MHC class I antibodies (clones 34-1-2s and AF6-88.5.5.3), injected with either isotype control antibody or anti-OPN antibody, and depleted or not of macrophages (A). Lung W/D weight ratios (B,D) and percentage of pulmonary PMNs (C) in C57BL/6 WT mice primed with LPS, depleted of CD4<sup>+</sup> T cells, injected with anti-MHC class I antibodies (clones 34-1-2s and AF6-88.5.5.3) and either cystamine or not (B,C) or anti-CD44 antibody or isotype antibody (D). Statistical analysis was performed with 1-way ANOVA with a Tukey post hoc test (A) or with 1-tailed unpaired Student t test (B-D). Each dot represents 1 mouse, and error bars represent SD. \* $P < .05$ , \*\* $P < .01$ , \*\*\*\* $P < .0001$ .

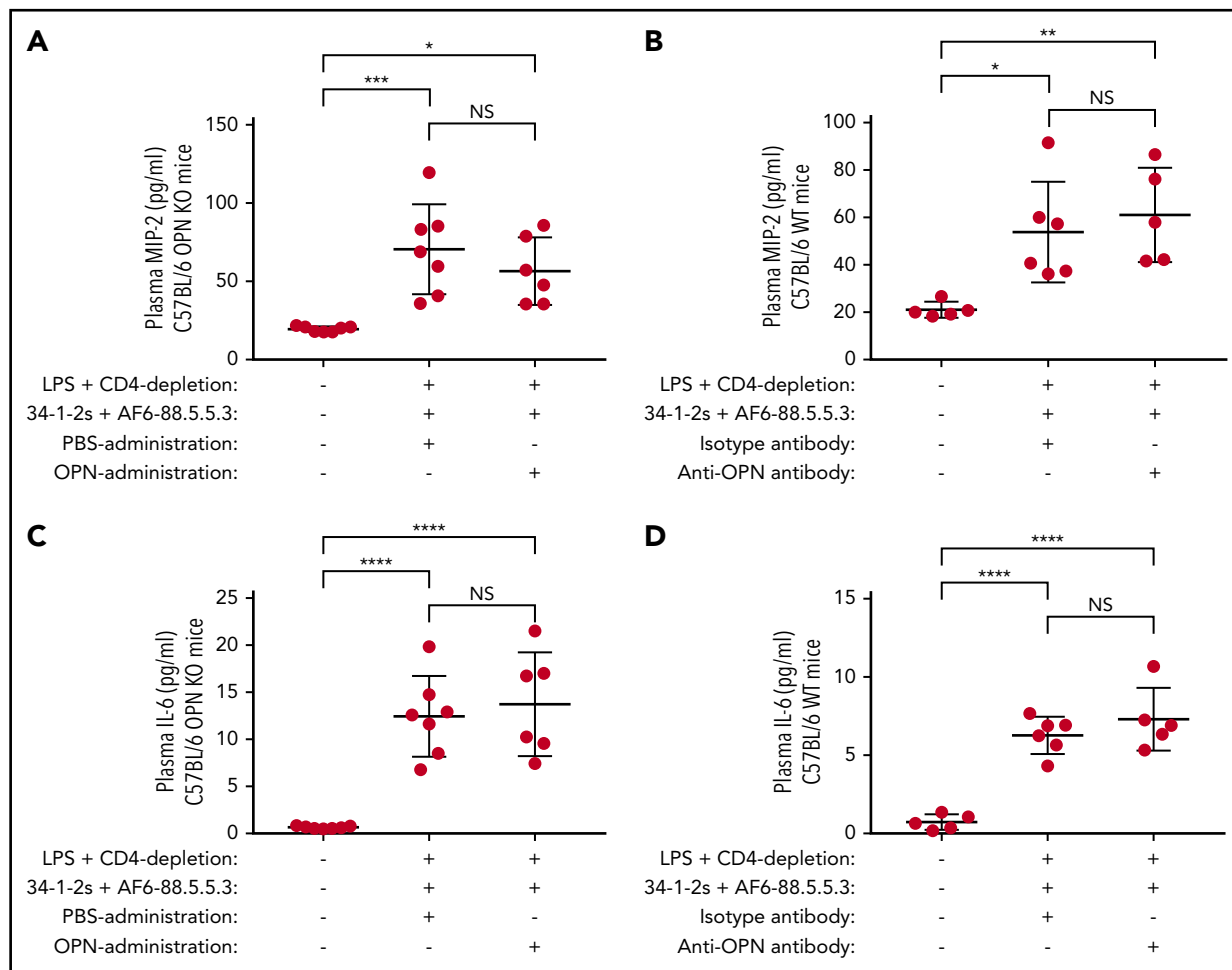


**Figure 7. Plasma MIP-2 or IL-6 levels do not change upon OPN-mediated TRALI induction or prevention.** Plasma MIP-2 levels (A-B) or IL-6 levels (C-D) in C57BL/6 OPN KO (A,C) or C57BL/6 WT mice (B,D) primed with LPS, depleted of CD4<sup>+</sup> T cells and injected with anti-MHC class I antibodies (clones 34-1-2s and AF6-88.5.5.3) and either with PBS or OPN (A,C) or isotype control antibody or anti-OPN antibody (B,D). For statistical analyses, only significant comparisons of interest are shown. Statistical analysis was performed with 1-way ANOVA with a Tukey post hoc test. Each dot represents 1 mouse, and error bars represent SD. \**P* < .05, \*\*\**P* < .01, \*\*\*\**P* < .001, \*\*\*\*\**P* < .0001.

G-CSF, KC, MCP-1, MIP-1 $\alpha$ , MIP-1 $\beta$ , RANTES, and TNF $\alpha$  (supplemental Figure 4a,b,d-i). Importantly, however, administration of OPN did not affect any of the tested chemoattractants (supplemental Figure 4), indicating independence of these cytokines from the effects induced by OPN. Similarly, in the WT mice injected with TRALI antibodies, significantly increased plasma levels of G-CSF, MCP-1, KC, MIP-1 $\alpha$ , MIP-1 $\beta$ , and RANTES were observed compared with naive control mice (supplemental Figure 5b,d-h). Although treatment with anti-OPN antibody further increased the levels of KC and MIP-1 $\alpha$  (supplemental Figure 5e-f), none of the investigated cytokines decreased (supplemental Figure 5). These cytokine data are summarized in supplemental Table 1.

## Discussion

Although the pathophysiology of TRALI is incompletely understood, PMNs are assumed to be the major pathogenic cells mediating lung damage based on both human autopsy reports and animal models.<sup>1-3</sup> The critical involvement of PMNs in the induction TRALI has been illustrated by murine studies where in vivo depletion of PMNs was shown to result in complete protection from antibody-mediated TRALI.<sup>4,25,26</sup>

Mechanisms regulating PMN migration toward the lungs in TRALI have not been extensively investigated although multiple murine TRALI models have demonstrated that the PMN chemoattractant MIP-2 plays an important role in this process.<sup>4,13,20,23,24</sup> MIP-2 is the murine homolog of human IL-8, which has been shown to be increased in TRALI patients.<sup>9,10</sup> On the other hand, OPN is also recognized as a proinflammatory cytokine<sup>16</sup> and is one of the most abundantly expressed proteins in various pulmonary disorders including inflammatory, fibrotic, vascular, and malignant lung disorders.<sup>17</sup> In addition, OPN is a key cytokine involved in regulating the migration of immune cells,<sup>16</sup> particularly the recruitment and migration of PMNs.<sup>22</sup>

We therefore investigated the role of OPN in regulating pulmonary PMN recruitment in TRALI using a previously established anti-MHC class I antibody-mediated C57BL/6 mouse model of TRALI.<sup>4,20</sup> We found that in WT mice, TRALI occurred as expected, however, OPN KO mice were fully protected from TRALI development. Furthermore, injection of purified OPN into the OPN KO mice could restore the pathogenic TRALI response, whereas blocking OPN in WT mice with an anti-OPN antibody prevented the onset of TRALI. All of the OPN-induced TRALI responses were directly related to increased pulmonary PMN



recruitment, and the development of acute lung injury was verified by increased lung W/D weight ratios and lung tissue histology analysis. Inflammation is an important risk factor for TRALI development<sup>2</sup> and, importantly, OPN has been shown to be upregulated at sites of inflammation such as injured lung epithelium and inflamed vascular endothelium.<sup>27,28</sup> We therefore investigated and confirmed the presence of OPN in the lungs of TRALI mice through immunohistochemistry, with no specific detection of OPN upon LPS priming and CD4<sup>+</sup> T-cell depletion. The presence of OPN in the lungs coincided with pulmonary PMN accumulation and the occurrence of acute lung injury. Interestingly, the pulmonary presence of OPN during TRALI corresponded to low levels of OPN in the plasma during TRALI as well as to increased levels of plasma OPN upon TRALI prevention with anti-OPN antibody treatment. This suggests that the anti-OPN antibody may retain OPN in the plasma and prevents its migration toward the lungs during TRALI. This suggests that in antibody-mediated TRALI, OPN acts as a proinflammatory cytokine that localizes to the lungs where it recruits PMNs that have been previously shown to mediate lung injury via reactive oxygen species (ROS) production.<sup>4</sup>

PMNs are known to be poor producers of OPN,<sup>22</sup> and OPN is also not expressed in circulating monocytes but is dramatically upregulated during macrophage differentiation with OPN being one of the major factors produced by macrophages.<sup>29</sup> We therefore hypothesized that macrophages may be the cellular source of OPN in TRALI. We found that macrophages are indeed pathogenic in murine antibody-mediated PMN-dependent TRALI. Regarding OPN, we observed that macrophage depletion not only prevented pulmonary PMN accumulation and TRALI, but it also prevented increased levels of OPN in plasma, which we observed to occur when the TRALI response was blocked by anti-OPN antibody treatment in the presence of macrophages.

Of interest, OPN has been shown to undergo polymerization *in vivo*, which was found to be essential for the induction of PMN chemotaxis.<sup>30</sup> It was demonstrated that if OPN polymerizes *in vivo*, the plasma levels of intact OPN decrease compared with polymerization-incompetent OPN.<sup>30</sup> Thus, in the TRALI experiments, where anti-OPN-blocking antibody was infused to prevent pulmonary PMN accumulation and TRALI, it may have inhibited OPN polymerization leading to a disruption of the PMN-chemotactic signal and increased levels of intact OPN in the plasma. Of interest, anti-OPN antibody treatment also attenuated PMN migration in a model of sepsis-induced acute lung injury.<sup>31</sup> Indeed, we found polymerization of OPN to be required for the induction of antibody-mediated PMN-dependent TRALI, as administration of cystamine, a transglutaminase inhibitor known to block polymerization *in vivo*,<sup>30</sup> prevented pulmonary PMN accumulation and the onset of TRALI.

OPN is able to interact with many cell types via various cell surface receptors, including CD44.<sup>32</sup> As the CD44 family of surface receptors regulates adhesion and migration and is one of the major receptors for OPN, we investigated its contribution in mediating TRALI. We blocked CD44 in the TRALI mouse model using an anti-CD44 antibody, but we found that this did not affect the occurrence of TRALI. Alternatively, OPN has been

shown to interact with a large variety of integrins, including  $\alpha v \beta 1$ ,  $\alpha v \beta 3$ ,  $\alpha v \beta 5$ ,  $\alpha v \beta 6$ ,  $\alpha 8 \beta 1$ ,  $\alpha 5 \beta 1$ ,  $\alpha 9 \beta 1$ , and  $\alpha 4 \beta 7$ .<sup>33-40</sup> Interestingly, polymeric OPN was demonstrated to function as a potent PMN chemoattractant and was shown to interact with integrin  $\alpha 9 \beta 1$  on PMNs.<sup>41</sup> Subsequent research will establish whether, during TRALI, OPN may be interacting with integrins.

Our and other studies have described OPN as being important for the recruitment and migration of PMNs, whereas other neutrophil functions such as phagocytosis and generation of ROS are described as not being affected by OPN.<sup>22</sup> In TRALI, it appears that OPN critically recruits PMNs to the lungs and, previously, we showed the critical requirement for PMNs and ROS (using gp91phox KO mice) in antibody-mediated TRALI induction.<sup>4</sup> Priming by OPN of neutrophil functions such as ROS production, however, cannot be excluded.

We found that plasma MIP-2 and IL-6 levels were increased in mice that were infused with anti-MHC class I antibodies as compared with naive controls but administration or blocking of OPN did not affect these MIP-2 or IL-6 levels. Thus, OPN appears to be a novel factor regulating pulmonary PMN recruitment and TRALI induction, which is not only critically required but also appears to be functioning independently of MIP-2 and IL-6. We also investigated the effect of OPN administration on other cytokines that have been described to be able to promote PMN chemotaxis (GM-CSF, G-CSF, interferon- $\gamma$ , KC, MCP-1, MIP-1 $\alpha$ , MIP-1 $\beta$ , RANTES, and TNF- $\alpha$ ).<sup>42-50</sup> None of these cytokines were increased by the administration of OPN, indicating that the pulmonary PMN recruitment and TRALI induction by OPN are distinct mechanisms. This was further supported by demonstrating that these cytokines were not affected in mice where the TRALI response was blocked by infusion of the anti-OPN antibody. None of these cytokines demonstrated decreased levels upon anti-OPN antibody treatment, which prevented the occurrence of pulmonary PMN recruitment and TRALI induction.

Collectively, these data indicate OPN as a novel and critical pathogenic factor that enhances antibody-mediated murine TRALI through stimulation of PMN migration toward the lungs independently of MIP-2, IL-6, or other PMN attractants. This suggests that blocking OPN (using an anti-OPN antibody) may prevent TRALI by impairing pulmonary PMN accumulation, and this should be explored as a potential therapeutic strategy to combat this serious adverse complication of blood transfusion.

## Acknowledgments

This work was supported by grants from Lund University, Crafoordska Stiftelsen (#20170829), Vetenskapsrådet (Swedish Research Council, VR, #2017-01779), and Avtal om Läkarutbildning och Forskning (ALF).

## Authorship

Contribution: R.K. designed and performed experiments, collected, analyzed, and interpreted data, and wrote and edited the paper; G.K. and J.R. performed experiments and collected data; A.E. supplied OPN KO mice and edited the manuscript; and J.W.S. provided financial resources and edited the manuscript.

Conflict-of-interest disclosure: The authors declare no competing financial interests.

The current affiliation for R.K. is Department of Experimental Immunohematology, Sanquin Research, and Landsteiner Laboratory, Amsterdam UMC, University of Amsterdam, Amsterdam, The Netherlands.

The current affiliation for G.K. is Bioscience COPD/IPF, Early Respiratory, Inflammation and Autoimmunity, R&D Biopharmaceuticals, Gothenburg, Sweden.

ORCID profiles: R.K., 0000-0002-1608-876X; G.K., 0000-0001-7552-9708; J.W.S., 0000-0002-1510-0077.

Correspondence: John W. Semple, Lund University, BMC C14, Klinikgatan 26, 221 84, Lund, Sweden; e-mail: john\_w.semble@med.lu.se.

## Footnotes

Submitted 4 April 2019; accepted 2 May 2019. Prepublished online as *Blood* First Edition paper, 10 May 2019; DOI 10.1182/blood.2019000972.

Presented as an oral abstract at the 60th annual meeting and exposition of the American Society of Hematology, San Diego, CA, 1-4 December 2018.

The online version of this article contains a data supplement.

There is a *Blood* Commentary on this article in this issue.

The publication costs of this article were defrayed in part by page charge payment. Therefore, and solely to indicate this fact, this article is hereby marked "advertisement" in accordance with 18 USC section 1734.

## REFERENCES

1. Semple JW, Rebetz J, Kapur R. Transfusion-associated circulatory overload and transfusion-related acute lung injury. *Blood*. 2019;133(17):1840-1853.
2. Semple JW, McVey MJ, Kim M, Rebetz J, Kuebler WM, Kapur R. Targeting transfusion-related acute lung injury: the journey from basic science to novel therapies. *Crit Care Med*. 2018;46(5):e452-e458.
3. Rebetz J, Semple JW, Kapur R. The pathogenic involvement of neutrophils in acute respiratory distress syndrome and transfusion-related acute lung injury. *Transfus Med Hemother*. 2018;45(5):290-298.
4. Kapur R, Kim M, Aslam R, et al. T regulatory cells and dendritic cells protect against transfusion-related acute lung injury via IL-10. *Blood*. 2017;129(18):2557-2569.
5. Silliman CC, Paterson AJ, Dickey WO, et al. The association of biologically active lipids with the development of transfusion-related acute lung injury: a retrospective study. *Transfusion*. 1997;37(7):719-726.
6. Silliman CC. The two-event model of transfusion-related acute lung injury. *Crit Care Med*. 2006;34(suppl 5):S124-S131.
7. Peters AL, Van Stein D, Vlaar AP. Antibody-mediated transfusion-related acute lung injury; from discovery to prevention. *Br J Haematol*. 2015;170(5):597-614.
8. Peters AL, van Hezel ME, Juffermans NP, Vlaar AP. Pathogenesis of non-antibody mediated transfusion-related acute lung injury from bench to bedside. *Blood Rev*. 2015;29(1):51-61.
9. Roubinian NH, Looney MR, Kor DJ, et al; TRALI Study Group. Cytokines and clinical predictors in distinguishing pulmonary transfusion reactions. *Transfusion*. 2015;55(8):1838-1846.
10. Vlaar AP, Hofstra JJ, Determann RM, et al. Transfusion-related acute lung injury in cardiac surgery patients is characterized by pulmonary inflammation and coagulopathy: a prospective nested case-control study. *Crit Care Med*. 2012;40(10):2813-2820.
11. Kapur R, Kim M, Rondina MT, Porcelijn L, Semple JW. Elevation of C-reactive protein levels in patients with transfusion-related acute lung injury. *Oncotarget*. 2016;7(47):78048-78054.
12. Pepys MB, Hirschfield GM. C-reactive protein: a critical update. *J Clin Invest*. 2003;111(12):1805-1812.
13. Kapur R, Kim M, Shanmugabhavanathan S, Liu J, Li Y, Semple JW. C-reactive protein enhances murine antibody-mediated transfusion-related acute lung injury. *Blood*. 2015;126(25):2747-2751.
14. Icer MA, Gezmen-Karadag M. The multiple functions and mechanisms of osteopontin. *Clin Biochem*. 2018;59:17-24.
15. Wesson JA, Johnson RJ, Mazzali M, et al. Osteopontin is a critical inhibitor of calcium oxalate crystal formation and retention in renal tubules. *J Am Soc Nephrol*. 2003;14(1):139-147.
16. Lund SA, Giachelli CM, Scatena M. The role of osteopontin in inflammatory processes. *J Cell Commun Signal*. 2009;3(3-4):311-322.
17. O'Regan A. The role of osteopontin in lung disease. *Cytokine Growth Factor Rev*. 2003;14(6):479-488.
18. Liaw L, Birk DE, Ballas CB, Whitsitt JS, Davidson JM, Hogan BL. Altered wound healing in mice lacking a functional osteopontin gene (spp1). *J Clin Invest*. 1998;101(7):1468-1478.
19. O'Brien ER, Garvin MR, Stewart DK, et al. Osteopontin is synthesized by macrophage, smooth muscle, and endothelial cells in primary and restenotic human coronary atherosclerotic plaques. *Arterioscler Thromb*. 1994;14(10):1648-1656.
20. Kapur R, Kim M, Rebetz J, et al. Gastrointestinal microbiota contributes to the development of murine transfusion-related acute lung injury. *Blood Adv*. 2018;2(13):1651-1663.
21. Matute-Bello G, Downey G, Moore BB, et al; Acute Lung Injury in Animals Study Group. An official American Thoracic Society workshop report: features and measurements of experimental acute lung injury in animals. *Am J Respir Cell Mol Biol*. 2011;44(5):725-738.
22. Koh A, da Silva AP, Bansal AK, et al. Role of osteopontin in neutrophil function. *Immunology*. 2007;122(4):466-475.
23. Fung YL, Kim M, Tabuchi A, et al. Recipient T lymphocytes modulate the severity of antibody-mediated transfusion-related acute lung injury. *Blood*. 2010;116(16):3073-3079.
24. McKenzie CG, Kim M, Singh TK, Milev Y, Freedman J, Semple JW. Peripheral blood monocyte-derived chemokine blockade prevents murine transfusion-related acute lung injury (TRALI). *Blood*. 2014;123(22):3496-3503.
25. Looney MR, Su X, Van Ziffle JA, Lowell CA, Matthay MA. Neutrophils and their Fc gamma receptors are essential in a mouse model of transfusion-related acute lung injury. *J Clin Invest*. 2006;116(6):1615-1623.
26. Looney MR, Nguyen JX, Hu Y, Van Ziffle JA, Lowell CA, Matthay MA. Platelet depletion and aspirin treatment protect mice in a two-event model of transfusion-related acute lung injury. *J Clin Invest*. 2009;119(11):3450-3461.
27. O'Regan AW, Chupp GL, Lowry JA, Goetschkes M, Mulligan N, Berman JS. Osteopontin is associated with T cells in sarcoid granulomas and has T cell adhesive and cytokine-like properties in vitro. *J Immunol*. 1999;162(2):1024-1031.
28. Nau GJ, Guilfoile P, Chupp GL, et al. A chemoattractant cytokine associated with granulomas in tuberculosis and silicosis. *Proc Natl Acad Sci USA*. 1997;94(12):6414-6419.
29. Krause SW, Rehli M, Kreutz M, Schwarzfischer L, Paulauskis JD, Andreesen R. Differential screening identifies genetic markers of monocyte to macrophage maturation. *J Leukoc Biol*. 1996;60(4):540-545.
30. Nishimichi N, Hayashita-Kinoh H, Chen C, Matsuda H, Sheppard D, Yokosaki Y. Osteopontin undergoes polymerization in vivo and gains chemotactic activity for neutrophils mediated by integrin alpha9-beta1. *J Biol Chem*. 2011;286(13):11170-11178.
31. Hirano Y, Aziz M, Yang WL, et al. Neutralization of osteopontin attenuates neutrophil migration in sepsis-induced acute lung injury. *Crit Care*. 2015;19(1):53.
32. Weber GF, Ashkar S, Glimcher MJ, Cantor H. Receptor-ligand interaction between CD44 and osteopontin (Eta-1). *Science*. 1996;271(5248):509-512.
33. Liaw L, Skinner MP, Raines EW, et al. The adhesive and migratory effects of osteopontin are mediated via distinct cell surface integrins. Role of alpha v beta 3 in smooth muscle cell migration to osteopontin in vitro. *J Clin Invest*. 1995;95(2):713-724.

34. Yokosaki Y, Tanaka K, Higashikawa F, Yamashita K, Eboshida A. Distinct structural requirements for binding of the integrins  $\alpha$ v $\beta$ 6,  $\alpha$ v $\beta$ 3,  $\alpha$ v $\beta$ 5,  $\alpha$ 5 $\beta$ 1 and  $\alpha$ 9 $\beta$ 1 to osteopontin. *Matrix Biol.* 2005;24(6):418-427.
35. Denda S, Reichardt LF, Müller U. Identification of osteopontin as a novel ligand for the integrin  $\alpha$ 8 $\beta$ 1 and potential roles for this integrin-ligand interaction in kidney morphogenesis. *Mol Biol Cell.* 1998;9(6):1425-1435.
36. Hu DD, Lin EC, Kovach NL, Hoyer JR, Smith JW. A biochemical characterization of the binding of osteopontin to integrins  $\alpha$ v $\beta$ 1 and  $\alpha$ v $\beta$ 5. *J Biol Chem.* 1995;270(44):26232-26238.
37. Yokosaki Y, Matsuura N, Sasaki T, et al. The integrin  $\alpha$ (9) $\beta$ (1) binds to a novel recognition sequence (SVVYGLR) in the thrombin-cleaved amino-terminal fragment of osteopontin. *J Biol Chem.* 1999;274(51):36328-36334.
38. Ito K, Kon S, Nakayama Y, et al. The differential amino acid requirement within osteopontin in  $\alpha$ 4 and  $\alpha$ 9 integrin-mediated cell binding and migration. *Matrix Biol.* 2009;28(1):11-19.
39. Green PM, Ludbrook SB, Miller DD, Horgan CM, Barry ST. Structural elements of the osteopontin SVVYGLR motif important for the interaction with  $\alpha$ (4) integrins. *FEBS Lett.* 2001;503(1):75-79.
40. Bayless KJ, Davis GE. Identification of dual  $\alpha$ 4 $\beta$ 1 integrin binding sites within a 38 amino acid domain in the N-terminal thrombin fragment of human osteopontin. *J Biol Chem.* 2001;276(16):13483-13489.
41. Nishimichi N, Higashikawa F, Kinoh HH, Tateishi Y, Matsuda H, Yokosaki Y. Polymeric osteopontin employs integrin  $\alpha$ 9 $\beta$ 1 as a receptor and attracts neutrophils by presenting a de novo binding site. *J Biol Chem.* 2009;284(22):14769-14776.
42. Gomez-Cambronero J, Horn J, Paul CC, Baumann MA. Granulocyte-macrophage colony-stimulating factor is a chemoattractant cytokine for human neutrophils: involvement of the ribosomal p70 S6 kinase signaling pathway. *J Immunol.* 2003;171(12):6846-6855.
43. Yong KL. Granulocyte colony-stimulating factor (G-CSF) increases neutrophil migration across vascular endothelium independent of an effect on adhesion: comparison with granulocyte-macrophage colony-stimulating factor (GM-CSF). *Br J Haematol.* 1996;94(1):40-47.
44. Bonville CA, Percopo CM, Dyer KD, et al. Interferon-gamma coordinates CCL3-mediated neutrophil recruitment in vivo. *BMC Immunol.* 2009;10:14.
45. De Filippo K, Henderson RB, Laschinger M, Hogg N. Neutrophil chemokines KC and macrophage-inflammatory protein-2 are newly synthesized by tissue macrophages using distinct TLR signaling pathways. *J Immunol.* 2008;180(6):4308-4315.
46. Balamayooran G, Batra S, Balamayooran T, Cai S, Jeyaseelan S. Monocyte chemoattractant protein 1 regulates pulmonary host defense via neutrophil recruitment during *Escherichia coli* infection. *Infect Immun.* 2011;79(7):2567-2577.
47. Ramos CD, Canetti C, Souto JT, et al. MIP-1 $\alpha$ [CCL3] acting on the CCR1 receptor mediates neutrophil migration in immune inflammation via sequential release of TNF- $\alpha$  and LT $\beta$ 4. *J Leukoc Biol.* 2005;78(1):167-177.
48. Bless NM, Huber-Lang M, Guo RF, et al. Role of CC chemokines (macrophage inflammatory protein-1  $\beta$ , monocyte chemoattractant protein-1, RANTES) in acute lung injury in rats. *J Immunol.* 2000;164(5):2650-2659.
49. Pan ZZ, Parkyn L, Ray A, Ray P. Inducible lung-specific expression of RANTES: preferential recruitment of neutrophils. *Am J Physiol Lung Cell Mol Physiol.* 2000;279(4):L658-L666.
50. Lukacs NW, Strieter RM, Chensue SW, Widmer M, Kunkel SL. TNF- $\alpha$  mediates recruitment of neutrophils and eosinophils during airway inflammation. *J Immunol.* 1995;154(10):5411-5417.